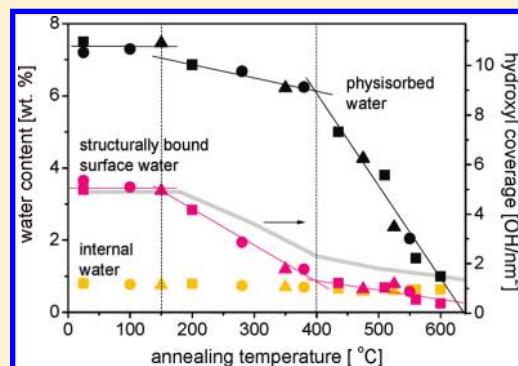


Three Regimes of Water Adsorption in Annealed Silica Opals and Optical Assessment

Francisco Gallego-Gómez,* Alvaro Blanco, Dolores Golmayo, and Cefe López

Instituto de Ciencia de Materiales de Madrid, C/Sor Juana Inés de la Cruz 3, 28049 Madrid, Spain

ABSTRACT: Physisorbed and structurally bound (surface and internal) water in silica opals are distinguished and quantified by thermogravimetry. By controlled dehydroxylation with thermal annealing, we correlate these forms of water with the silica chemistry. In particular, we find that the silica capability to physically adsorb water from ambient moisture exhibits three regimes, associated with the distinct condensation behavior of bonded and unbonded surface silanols. Features in both opal IR absorbance and photonic band gap reproduce the physisorbed water regimes. This allows direct assessment of the water content and its evolution just by routine optical spectroscopy, being a useful tool for local and nondestructive analysis of colloidal silica. Besides, this provides a simple recipe for accurate tuning of the opal photonic band gap (about 10% in position and width) by just selecting the annealing temperature.



INTRODUCTION

Artificial opals,¹ solid colloidal crystals of self-assembled spheres, are inexpensive and versatile three-dimensional photonic crystals exhibiting a *photonic band gap* (PBG), in which light cannot propagate. Opals made of submicrometer silica spheres in a face centered cubic (fcc) package² are widely used because of the ease of fabrication. Their photonic properties (given by the PBG characteristics) depend on the size and packing of the spheres but also on the refractive indices of the materials forming the opal, that is, silica and the surrounding medium (air, in general). The abundant presence of silanol groups (Si–OH) at the colloidal silica surface makes spheres markedly hydrophilic. Water from moisture is physically adsorbed (*physisorbed water*) through hydrogen bonds to surface silanols, staying in the opal interstices and strongly affecting the opal properties.³ Additionally, the hydroxyl (–OH) groups of the silanols constitute *structurally bound water*⁴ on the spheres surface (surface silanols) and inside the silica skeleton (internal silanols).

Thermal annealing is known to modify the silica chemistry by progressive silanol condensation (dehydroxylation).⁵ Zhuravlev's model classically describes the silica state depending on the annealing temperature (T_a), distinguishing two stages.^{4,6,7} First, surface silanols begin to condense at ~ 200 °C (or even before, at 130 – 150 °C^{8–10}) and rapidly decrease until 400 °C, mainly due to the complete elimination of hydrogen-bonded (vicinal) silanols. Second, condensation of unbonded (geminal and free) silanols levels off until total dehydroxylation at ~ 1000 °C. Annealing makes silica gradually hydrophobic so less physisorbed water is expected. Internal silanol groups, less investigated, are estimated to undergo condensation above 600 °C.^{6,7,11} Upon both surface and internal silanol condensation, bound water is released, which can also affect the opal properties if the sphere morphology or refractive index changes. Finally, incipient sintering can begin at 600 – 700 °C.^{6,12,13}

Annealing at high temperature (~ 1000 °C) has usually been applied to silica opals to induce sintering and increase their mechanical strength. However, only a few authors^{13–16} have studied the annealing effect on the photonic properties before sintering. They observed PBG permanent changes (namely, shifts to shorter wavelengths), ascribed to an overall water decrease. Nevertheless, the water (physisorbed and bound) present in the annealed opals, and its correlation with the PBG changes, was not investigated. On the other hand, while the physicochemistry of silanols has been extensively investigated in many silica types, much less has been reported on the associated water (e.g., dependence on annealing, relationship between physisorbed water and surface silanol types, internal water content).

Here we subject silica opals to thermal treatment for controlled modification of the spheres' surface chemistry ($T_a \leq 600$ °C to safely avoid the initial stage of sintering, i.e., formation of silica necks between spheres and change of the specific surface). Annealing effects are analyzed attending not only to the optical properties changes but also to the water (form and content) in the opals after treatment. Four aims were pursued: (1) distinction and quantification of the different forms of water and their dependence on the silica dehydroxylation, (2) correlation of the physisorbed water content with the chemistry of the silica surface, (3) alternative measurement of water in silica by optical means, allowing nondestructive and local analysis, and (4) simple procedure for accurate tuning of the opal PBG properties by thermal annealing. Thermogravimetry and optical spectroscopy were used in this study.

Received: September 8, 2011

Revised: October 27, 2011

Published: October 31, 2011

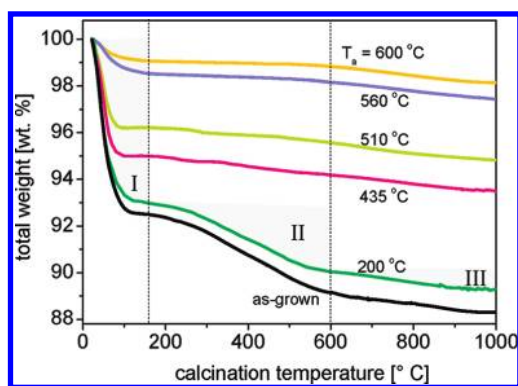


Figure 1. TGA curves of as-grown (black line) and annealed ($T_a = 200$ – 600 °C, color lines) silica opals ($D = 335$ nm). Shaded areas (I–III), depicted only for the 200 °C annealed opal, correspond to physisorbed, structurally bound surface and internal water (see text).

EXPERIMENTAL SECTION

Opal Fabrication and Thermal Annealing. Artificial opals were prepared from dilute ethanol colloidal suspensions of monosized Stöber silica spheres¹⁷ (with diameter D of 230, 280, or 335 nm, 3% polydispersity) following the vertical deposition method under controlled temperature and humidity conditions.³ The resulting opals had an average size of >2 μm^2 and were formed by ~ 30 monolayers. As-grown opals were annealed in air at different T_a between 100 and 600 °C in a conventional oven by slowly heating (1 °C/min) up to T_a , waiting for 3 h, and then cooling down to room temperature (10 °C/min).

Thermal Gravimetric Analysis (TGA). TGA was performed by using a Mettler Toledo TGA/DSC 1 instrument on as-grown and annealed opals after detaching from the glass substrate. Samples (7–10 mg in each case) were heated in static air atmosphere from room temperature to 1000 °C (5 °C/min).

Visible–IR Spectroscopy. Optical characterization was performed on a small area (~ 20 μm^2) using a Fourier transform infrared spectrometer (Bruker IFS 66S) with a microscope attached. IR optical transmittance was used to measure the broad absorption band centered at ~ 3 μm , corresponding to O–H stretching bands of hydrogen-bonded molecular water and SiO–H stretching of surface silanols bonded to molecular water.^{6,18} Visible–NIR reflectance spectra were used to characterize the opal PBG.

PBG Properties. Photonic properties were inferred from the position and width of the Bragg peak (the lowest energy PBG, associated to the diffraction at the (111) family of planes). Its position (λ_{Bragg}) is described in a good approximation by Bragg's law, given at normal incidence by

$$\lambda_{\text{Bragg}} = 2d_{111}\sqrt{fn_p^2 + (1-f)n_v^2} \quad (1)$$

where the lattice parameter d_{111} is the spacing of the (111) planes, f is the filling fraction of the silica spheres (of refractive index n_p), and n_v is the average refractive index of the opal voids depending on the media filling them, that is, relative amounts of air and water.³ The experimental PBG width was obtained from the full-width at half-maximum (fwhm) of the Bragg peak.

RESULTS AND DISCUSSION

Before measurements, as grown and annealed samples were stored under ambient conditions (22 °C, $\sim 35\%$ humidity) for at least 1 day to allow complete moisture adsorption. Nevertheless, no dependence on storage time between several hours and few weeks was observed. Opal high quality was preserved after thermal treatment as the maximum reflectance values ($\sim 80\%$)

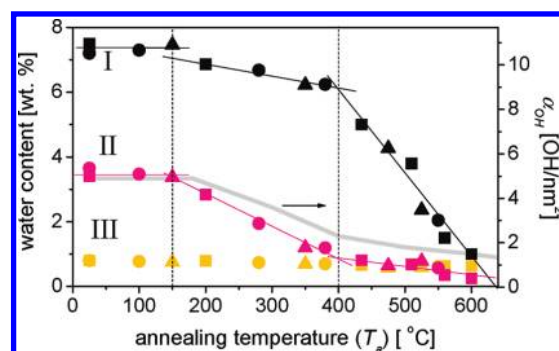


Figure 2. Dependence on the thermal treatment of water contents corresponding to regions I–III of TGA (Figure 1). Data were obtained in opals made of silica spheres of $D = 335$, 280, and 230 nm (squares, circles, and triangles, respectively). Solid lines are a guide to the eye. Dashed lines signify the three regimes of water adsorption (see text). For the sake of comparison, the hydroxyl coverage (α_{OH}) is also plotted (gray curve, right axis); data from ref 5.

barely decreased. No discernible sphere deformation or sintering was observed by scanning electron microscopy. In general, opal cracks or disorder did not significantly increase upon annealing (otherwise, the sample was discarded).

TGA through weight loss upon calcination yielded the total amount of water in each opal assuming complete silica desiccation at 1000 °C.^{11,13,19} Figure 1 shows the overall weight loss drastically diminishing in annealed opals with increasing T_a . Total water content in as-grown opals was around 12 wt % (consistent with previous work^{3,20,21}) and decreased to 2 wt % in those treated at 600 °C. The temperature-dependent behavior was similar in all cases and allowed us to distinguish three regions related to the different forms of water: an abrupt drop-off ending with a plateau at 120–180 °C (region I), which corresponds to desorption of all the physisorbed water; a moderate loss region until 600 °C (region II) due to removal of structurally bound water upon surface dehydroxylation; and a final weight loss above 600 °C (region III) mainly due to removal of internal water (i.e., condensation of internal silanols). By the latter assumption, we neglect the contribution of condensation of the remaining surface silanols, which is expected to be small.^{4,7}

From these considerations, we distinguish the three different forms of water (I–III) contained in as-grown and annealed opals, obtaining their dependence on the treatment temperature (Figure 2). Physisorbed water (I), being the largest fraction, reduced from ~ 8 wt % in as-grown opals to 1 wt % in samples annealed at 600 °C. Surface bound water (II) represented ~ 3.6 wt % of the as-grown films and practically disappeared after treatment. On the contrary, internal bound water (III), which was found to constitute the smallest fraction in as-grown opals (~ 0.8 wt %), barely decreased with T_a . This indicates that no significant internal silanol condensation occurred at $T_a \leq 600$ °C, as presumed.

As mentioned above, separate estimates of physisorbed and structurally bound water can hardly be found in the literature. Reported contents of physisorbed water (I) of 5–10 wt % in as-grown silica^{3,13,22} agree well with our results. Rather than on direct quantification of the structurally bound water, studies have focused on measuring the silanol density. Surface bound water (II) is associated to the surface silanol density (or hydroxyl coverage, α_{OH}), extensively investigated in as-grown and annealed silica.^{4–7} This allows no quantitative comparison with the water content but with its evolution against T_a (Figure 2),

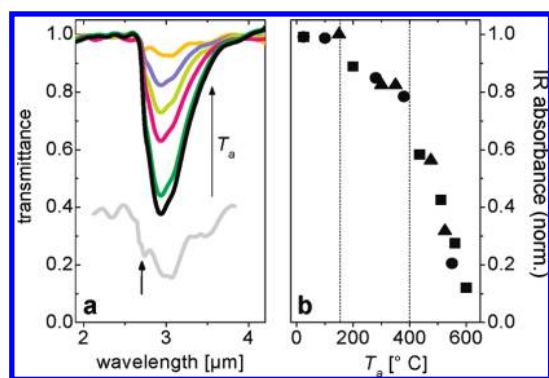


Figure 3. (a) IR transmission spectra of as-grown and annealed silica opals ($D = 335$ nm). Gray curve is the magnified spectrum (in arbitrary units) of the 600 °C annealed opal (the arrow points the peak at 3650 cm^{-1}). (b) IR absorbance ($1 - \text{transmittance}$) at 3 μm as function of the annealing temperature T_a . Absorbance was normalized to avoid dependence on the opal thickness. Color and symbol code is described in Figure 2.

showing a fair agreement. Some discrepancy is not surprising given the typical dispersion of α_{OH} in silicas (close to ± 1 OH/ nm^2). Besides, Figure 2 shows that, unexpectedly, physisorbed water would vanish at nonzero silanol density. This suggests that annealed silica opals possess somewhat less silanols, with faster condensation of vicinal silanols (200 – 400 °C), than average silica. The actual silanol density can be simply estimated by the experimental data of II read on the right axis. Regarding internal water (III), literature values can only be indirectly obtained from studies on the accessibility of small molecules to silanols. The reported fractions of 8 – 23% of silanols being inaccessible to D_2O (refs 7 and 22–25) are compatible with our internal water estimate, being 18% of the total structural water. No systematic investigation on the annealing-dependence of physisorbed or internal water has previously been reported.

Three regimes can be recognized in Figure 2, closely related to the above-described evolution with T_a of the surface chemistry. The first regime, up to $T_a \sim 150$ °C, corresponded to constant water contents since silanol condensation did not begin. Along the two further regimes, physisorbed water (I) and surface bound water (II) decreased at different rates. As mentioned above, the latter resembled the two-stage behavior of α_{OH} , with faster (mainly vicinal) silanol condensation up to $T_a \sim 400$ °C. By contrast, sphere hydrophilicity did not reduce proportionally, since physisorbed water barely decreased after treatment at $T_a = 200$ – 400 °C but strongly diminished after annealing at higher temperatures. This indicates that the adsorption (rehydration) capability was affected by the elimination of geminal and free silanols rather than of vicinal ones. This fully agrees with the energetic heterogeneity of the silica surface. Thus, vicinal (bonded) silanols are known to be low-energy adsorption sites while the adsorptivity of unbonded (in particular, free) silanols is much higher.^{6,22,26–28} This coincides with Zhuravlev's model distinguishing two regions (with inflection at 400 °C) for silica rehydroxylation (chemisorption), related, in turn, to a notable increase of the activation energy of desorption (E_D) observed after elimination of the vicinal silanols.^{4,7} In this context, the abrupt reduction of physisorbed water between $T_a = 150$ and 200 °C might be attributed to the sharp decrease of E_D at the transition from dehydration to dehydroxylation reported by Gillis-D'Hamers et al.^{6,27} Such a step is also notorious in Zhuravlev's results for E_D around 190 °C.⁴

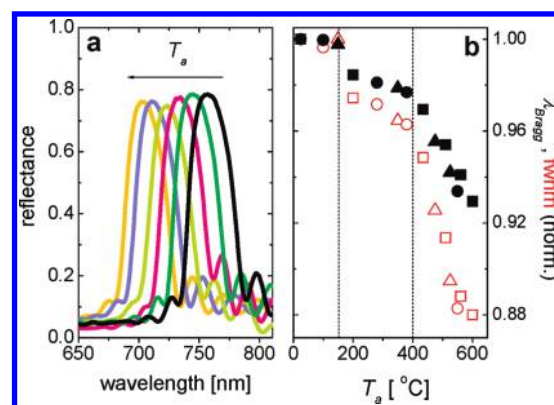


Figure 4. (a) Bragg peak reflectance of as-grown and annealed silica opals ($D = 335$ nm). (b) Change in both Bragg peak position (solid black symbols) and width (open red symbols) as function of the annealing temperature T_a . Data are normalized to the as-grown opal values in order to compare opals with different spheres size. Color and symbol code is described in Figure 2.

Despite the merits of TGA, its shortcomings are important: it is destructive, needs large amounts of sample (several milligrams), and provides only average information of the whole opal. Thus, optical analysis is a desirable alternative as a nondestructive technique suitable for very small opal areas. On the one hand, IR optical transmittance provides information about the water contained in the opals by measuring the absorption band at ~ 3 μm (Figure 3a). The absorbance gradually decreased (transmittance increased) in opals by increasing T_a , corresponding to less water in the annealed opals. Above $T_a = 500$ °C, the peak at ~ 3650 cm^{-1} (2.74 μm) associated to the internal $-\text{OH}$ groups^{7,28} became observable as physisorbed and surface bound water progressively disappeared. The IR absorbance (taken, e.g., at 3 μm) reproduced the dependence on T_a of the physisorbed water (the most abundant form), being sensitive to the inflection points at 150 and 400 °C and to the step between 150 and 200 °C (Figure 3b).

On the other hand, hydrophobicity is expected to affect the PBG properties as less physisorbed water fills the opal voids (smaller n_v) leading to a λ_{Bragg} decrease (eq 1). In fact, reflectance spectroscopy showed a clear PBG shift to shorter wavelengths in annealed opals (Figure 4a). Both the PBG position and width significantly decreased with T_a (up to 8 and 12% , respectively), resembling again the three well-defined regimes of the physisorbed water and the step at 150 °C (Figure 4b). Interestingly, abrupt PBG change right after heating above 150 °C was previously observed,^{3,13} although no satisfactory explanation was given. Note also that the band gap narrowing after annealing unambiguously indicates that the opal gradually tended from non-close- to close-packed structures, as less physisorbed water led to approximation between the spheres.³

Both opal IR absorbance and PBG change (in position and width) showed a linear relationship with the amount of physisorbed water, independently of the opal sphere size (Figure 5). Such a well-behaved trend enables, on the one hand, accurate tuning of the opal photonic properties just by selecting T_a . On the other hand, it permits estimation of the amount of water just by simple optical spectroscopy, being even sensitive to the different phases of water adsorption. This offers an advantageous alternative to TGA for measuring water in colloidal crystals. In order to use the PBG properties, structural order (before and after annealing) is mandatory.

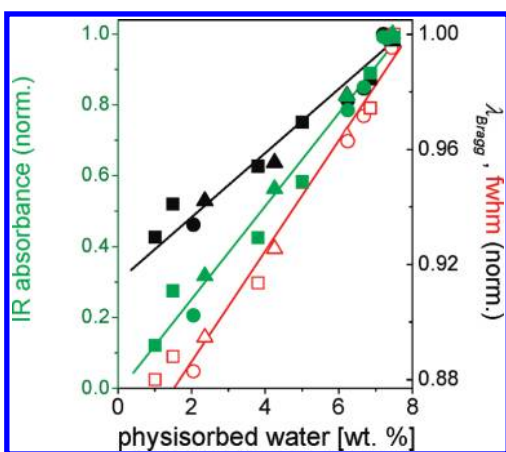


Figure 5. Correlation between optical spectroscopy data (normalized IR absorbance from Figure 3, green symbols; normalized PBG position and width from Figure 4, solid black and open red symbols, respectively) and the physisorbed water content (Figure 2) after annealing at different temperatures. Lines are linear regression fits.

CONCLUSIONS

The effect of annealing on the water content of silica artificial opals has been thoroughly investigated. Physisorbed and structurally bound (on the surface and internal) water was separately quantified by thermogravimetry. Upon annealing, surface bound water drastically decreased, as a result of silica surface dehydroxylation, while internal water only slightly reduced. Physisorbed water exhibited three regimes as a function of the treatment temperature, closely related to the energetic heterogeneity of silica surface. Water uptake capability (a) was unaffected after annealing below ~ 150 °C, (b) moderately decreased up to 400 °C, during (mainly) removal of bonded silanols, and (c) showed a pronounced reduction after annealing at higher temperatures, due to further condensation of unbonded silanols. The three-regime behavior was reproduced by routine optical spectroscopy (IR absorbance and Bragg peak features), being a reliable, nondestructive alternative to measure water properties. The well-behaved trends provided a simple recipe for accurate tuning of the opal photonic band gap (up to $\sim 10\%$ in position and width) by just selecting the annealing temperature.

AUTHOR INFORMATION

Corresponding Author

*E-mail: francisco.gallego@icmm.csic.es.

ACKNOWLEDGMENT

F.G.-G. was supported by the JAE Postdoctoral Program from the CSIC. This work was partially supported by EU FP7 NoE Nanophotonics4Energy Grant No. 248855, the Spanish MICINN CSD2007-0046 (Nanolight.es), MAT2009-07841 (GLUSFA), and Comunidad de Madrid S2009/MAT-1756 (PHAMA) projects.

REFERENCES

- (1) Galisteo-López, J. F.; Ibisate, M.; Sapienza, R.; Froufe-Pérez, L. S.; Blanco, A.; López, C. *Adv. Mater.* **2011**, *23*, 30.
- (2) Miguez, H.; Meseguer, F.; López, C.; Mifsud, A.; Moya, J. S.; Vazquez, L. *Langmuir* **1997**, *13*, 6009.

- (3) Gallego-Gómez, F.; Blanco, A.; Canalejas-Tejero, V.; López, C. *Small* **2011**, *7*, 1838.
- (4) Zhuravlev, L. T. *Colloids Surf., A* **1993**, *74*, 71.
- (5) Zhuravlev, L. T. *Langmuir* **1987**, *3*, 316.
- (6) Vansant, E. F.; Van Der Voort, P.; Vrancken, K. C. *Characterization and Chemical Modification of the Silica Surface*; Elsevier: Amsterdam, 1995.
- (7) Bergna, H. E.; Roberts, W. O. *Colloidal Silica: Fundamentals and Applications*; CRC Press: Boca Raton, FL, 2006.
- (8) Sindorf, D. W.; Maciel, G. E. *J. Phys. Chem.* **1983**, *87*, 5516.
- (9) Morrow, B. A. *Stud. Surf. Sci. Catal.* **1990**, *57A*, A161.
- (10) Carteret, C. *J. Phys. Chem. C* **2009**, *113*, 13300.
- (11) Garcia-Santamaria, F.; Miguez, H.; Ibisate, M.; Meseguer, F.; Lopez, C. *Langmuir* **2002**, *18*, 1942.
- (12) Vasconcelos, W. L.; DeHoff, R. T.; Hench, L. L. *J. Non-Cryst. Solids* **1990**, *121*, 124.
- (13) Miguez, H.; Meseguer, F.; López, C.; Blanco, A.; Moya, J. S.; Requena, J.; Mifsud, A.; Fornés, V. *Adv. Mater.* **1998**, *10*, 480.
- (14) Van Le, T.; Ross, E. E.; Velarde, T. R. C.; Legg, M. A.; Wirth, M. J. *Langmuir* **2007**, *23*, 8554.
- (15) Liu, K.; Schmedake, T. A.; Tsu, R. *Phys. Lett. A* **2008**, *372*, 4517.
- (16) Liu, Y.-P.; Yan, Z.-J.; Li, Z.-G.; Li, Q.-T.; Wang, Y.-Y. *Chin. Phys. Lett.* **2010**, *27*, 074205.
- (17) Stöber, W.; Fink, A.; Bohn, E. *J. Colloid Interface Sci.* **1968**, *26*, 62.
- (18) Brinker, C. J.; Scherer, G. W. *Sol–Gel Science. The Physics and Chemistry of Sol–Gel Processing*; Academic Press: New York, 1990; pp 581–585.
- (19) De Farias, R. F.; Airoidi, C. *J. Therm. Anal.* **1998**, *53*, 751.
- (20) Sacks, M. D.; Tseng, T.-Y. *J. Am. Ceram. Soc.* **1984**, *67*, 526.
- (21) Chabanov, A. A.; Jun, Y.; Norris, D. J. *Appl. Phys. Lett.* **2004**, *84*, 3573.
- (22) Burneau, A.; Barres, O.; Gallas, J. P.; Lavalley, J. C. *Langmuir* **1990**, *6*, 1364.
- (23) Morrow, B. A.; McFarlan, A. J. *Langmuir* **1991**, *7*, 1695.
- (24) Gallas, J.-P.; Goupil, J.-M.; Vimont, A.; Lavalley, J.-C.; Gil, B.; Gilson, J.-P.; Miserque, O. *Langmuir* **2009**, *25*, S825.
- (25) Chuang, I.-S.; Kinney, D. R.; Maciel, G. E. *J. Am. Chem. Soc.* **1993**, *115*, 8695.
- (26) Hertl, W.; Hair, M. L. *Nature* **1969**, *223*, 1150.
- (27) Gillis-D’Hammers, L.; Cornelissens, I.; Vrancken, K. C.; Van Der Voort, P.; Vansant, E. F.; Daelemans, F. *J. Chem. Soc., Faraday Trans* **1992**, *88*, 723.
- (28) Davydov, V. Ya. In *Adsorption on Silica Surfaces*; Papirer, E., Ed.; Marcel Dekker Inc.: New York, 2000; Chapter 4.